Article

# Supramolecular Properties of a Monocarboxylic Acid-Functionalized "Texas-Sized" Molecular Box

Ren-Tsung Wu, Xiaodong Chi, Takehiro Hirao, Vincent M. Lynch, and Jonathan L. Sessler

*J. Am. Chem. Soc.*, **Just Accepted Manuscript** • DOI: 10.1021/jacs.7b12957 • Publication Date (Web): 14 May 2018

# Supramolecular Properties of a Monocarboxylic Acid-Functionalized "Texas-Sized" Molecular Box

Ren-Tsung Wu,† Xiaodong Chi,† Takehiro Hirao,† Vincent M. Lynch,† and Jonathan L. Sessler*†‡

†Department of Chemistry, The University of Texas at Austin, Austin, Texas 78712-1224, United States.

‡Institute for Supramolecular and Catalytic Chemistry, Shanghai University, Shanghai 200444, China.

*KEYWORDS. Texas-sized molecular box, guest-tethered macrocycle, and stimuli-responsive self-assembly.*

**ABSTRACT:** A new carboxylic acid-functionalized "Texas-sized" molecular box **TxSB-$CO_2$H** has been prepared by combining two separate building blocks via an iodide-catalyzed macrocyclization reaction. A single crystal X-ray diffraction analysis revealed a paired "clip-like" dimer in the solid state. Concentration-dependent behavior is seen for samples of **TxSB-$CO_2$H** as prepared, as inferred from $^1$H NMR spectroscopic studies carried out in DMSO-$d_6$. However, in the presence of excess acid (1% by weight of deuterated trifluoracetic acid; TFA-$d_1$), little evidence of aggregation is seen in DMSO-$d_6$ except at the highest accessible concentrations. In contrast, the conjugate base form, **TxSB-$CO_2^-$**, produced in situ via the addition of excess triethylamine to DMSO-$d_6$ solutions of **TxSB-$CO_2$H**, acts as a self-complementary monomer that undergoes self-assembly to stabilize a formal oligomer ([**TxSB-$CO_2^-$**]$_n$) with a degree of polymerization of approximately 5-6 at a concentration of 70 mM. Evidence in support of the proposed oligomerization of **TxSB-$CO_2^-$** in solution and in the solid state came from one- and two-dimensional $^1$H NMR spectroscopy, X-ray crystallography, dynamic light scattering (DLS), and scanning electron microscopy (SEM). A series of solution-based analyses carried out in DMSO and DMSO-$d_6$ provide support for the notion that the self-assembled constructs produced from **TxSB-$CO_2^-$** are responsive to environmental stimuli, including exposure to the acetate anion (as its tetrabutylammonium, $TBA^+$, salt), changes in overall concentration, temperature, and protonation state. The resulting transformations are thought to reflect the reversible nature of the underlying noncovalent interactions. They also permit the stepwise interconversion between **TxSB-$CO_2$H** and [**TxSB-$CO_2^-$**]$_n$ via the sequential addition of triethylamine and TFA-$d_1$. The present work thus serves to illustrate how appropriately functionalized molecular box-type macrocycles may be used to develop versatile stimuli-responsive materials. It also highlights how aggregated forms seen in the solid state are not necessarily retained under competitive solution phase conditions.

## INTRODUCTION

Macrocyclic hosts and receptors have played a time-honored role in the development of supramolecular chemistry.[1–5] Within the subset of positively charged macrocycles, the tetracationic cyclobis(paraquat-*p*-phenylene) (**CBPQT**$^{4+}$), also known as the "blue box," and structurally related macrocycles, developed by Stoddart and coworkers, are arguably the most iconic.[5–9] The box-like geometry of **CBPQT**$^{4+}$ and the strong donor-acceptor interactions it and its congeners support have allowed a wide range of mechanically interlocked molecular architectures to be prepared; many have emerged as promising materials for use in applications as diverse as inter alia: (i) host-guest recognition and assembly,[9–11] (ii) artificial photosynthesis,[12,13] (iii) molecular electronics,[14,15] and (iv) molecular machines.[16,17] Inspired by the chemistry of **CBPQT**$^{4+}$, in 2010 our group designed and prepared a tetracationic imidazolium-based macrocycle **1**$^{4+}$ and, subsequently, several related systems, *e.g.*, **2**$^{4+}$–**4**$^{4+}$ (Scheme 1).[18–20] Since our first-generation molecular box **1**$^{4+}$ was found to display greater conformational flexibility and a larger central cavity size than the original blue box (**CBPQT**$^{4+}$),[5] it was referred to as a "Texas-Sized" molecular box in order to highlight its distinctive structural features.[18] To date, we have found that macrocycle **1**$^{4+}$ can interact with a variety of electron-rich neutral and anionic guests and stabilize threaded or interpenetrated pseudorotaxane complexes when exposed to selected aromatic carboxylate anions.[18–24] Further studies have also corroborated that pseudorotaxane monomers of [**1**$^{4+}$·mono-terephthalate anion] could self-associate and support the formation of pseudo-oligorotaxane superarchitectures at high concentrations in solution.[22,23] In the case of the pseudorotaxane monomers of [**1**$^{4+}$·2,6-naphthalenedicarboxylate dianion], higher order polyrotaxane chains could be stabilized in the solid state by introducing silver cations into the self-assembly process.[22,23] In order to explore further the self-assembly chemistry of the Texas-sized molecular box, we have now prepared a carboxyl-functionalized derivative termed "**TxSB-$CO_2$H**", as well as its conjugate base "**TxSB-$CO_2^-$**" (Scheme 1). As detailed below, **TxSB-$CO_2$H** and

**TxSB-$CO_2^-$** give rise to dramatically disparate architectures in solution and in the solid state.

Currently, supramolecular oligomers and polymers are receiving considerable attention due to their potential in developing stimuli-responsive, self-healing, and shape-memory materials.[25–28] To date, a number of macrocyclic receptors have been exploited as self-complementary monomers capable of affording desirable oligomeric and polymeric superstructures via "head-to-tail" self-assembly.[29–32] Such macrocycle-based monomers are commonly obtained by incorporating a macrocyclic host (head) with a guest unit (tail) tethered to the core. When designed appropriately, the head of one macrocycle may be used to bind a tail of another monomer via intermolecular host-guest interactions, thus supporting self-assembly. For instance, our group noted early on that monocarboxylate-functionalized sapphyrins (a class of pentapyrrolic macrocycles) self-associate to produce head-to-tail supramolecular dimers in organic media and in the solid state.[29] Fluoride anions act as inhibitors of the dimerization process by competing for the sapphyrin cavity in preference over the pendant carboxylate arm. More recently, Stoddart *et al.*[31] reported a self-complementary monomer comprising a π electron-rich tetrathiafulvalene guest chromophore linked to a **CBPQT**$^{4+}$ ring. This system was shown to dimerize into a [*c*2]daisy chain system and undergo dissociation and recombination in solution in a manner that was found to depend on the concentration, temperature, and the nature of the linker.[31,32] As a complement to these prior studies and in an effort to explore in greater detail the self-assembly features of the Texas-sized molecular box, **1**$^{4+}$, we have prepared the monocarboxylic acid-functionalized derivative, **TxSB-$CO_2$H** (Scheme 1). This system was chosen for study because carboxylate anions are known to bind well to **1**$^{4+}$. In addition, switching between the acid (**TxSB-$CO_2$H**) and base (**TxSB-$CO_2^-$**) forms might result in the formation of two very different species exhibiting, perhaps, distinct molecular topologies. Finally, the short distance between the macrocyclic moiety (head) and the carboxylic acid (tail) was expected to preclude direct intramolecular self-association since the head cannot "bite" its own tail.[28] In fact, as discussed below, noncovalent dimerization of **TxSB-$CO_2$H** takes place in the solid state, albeit not in the competitive solvent, dimethyl sulfoxide (DMSO). In contrast, evidence for the stabilization of self-assembled oligomers of **TxSB-$CO_2^-$** is seen both in DMSO and in the solid state. The formation of disparate architectures from ostensibly similar building blocks is expected to advance our understanding of molecular self-assembly and provide insights into the design features needed to produce environmentally responsive supramolecular polymers.[17,26,33–35] As detailed below, interconversion between the monomeric form and the self-assembled oligomer can be effected via the sequential addition of triethylamine (TEA) and deuterated trifluoracetic acid (TFA-$d_1$).

**SCHEME 1. (a) Synthetic route to TxSB$CO_2$H·4$PF_6$. (b) "Texas-sized" molecular box 1$^{4+}$ and the congeneric macrocyclic receptors 2$^{4+}$–4$^{4+}$.**

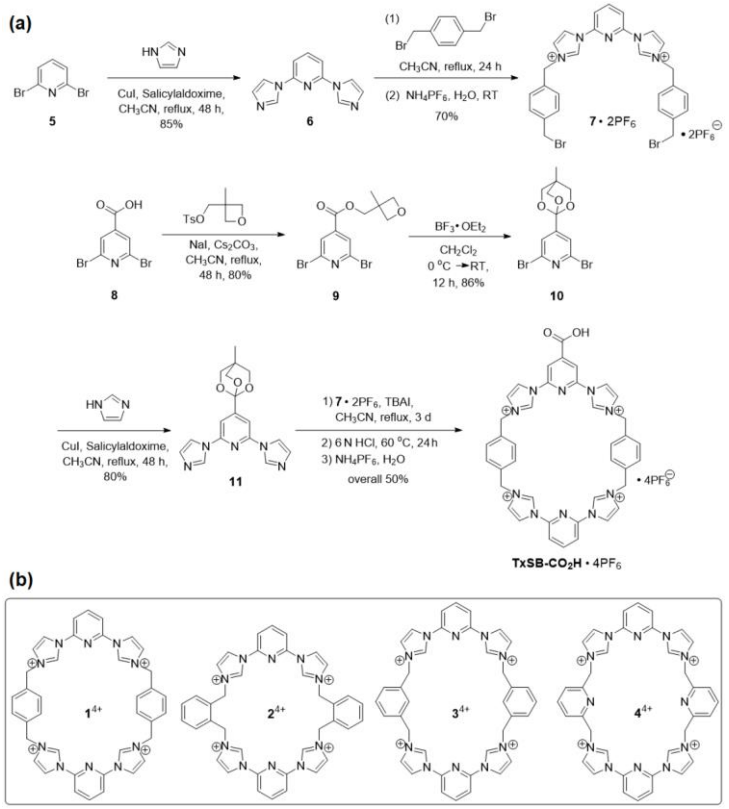

## RESULTS AND DISCUSSION

The synthesis of **TxSB-$CO_2$H** is summarized in Scheme 1. It relies on the coupling between two separate building blocks, namely **7**·2$PF_6$ and **11**. The acyclic dibromide **7**·2$PF_6$ was generated via an Ullmann-type coupling of the dibromopyridine **5** with imidazole to give diimidazolyl pyridine **6**.[36] Subsequent dialkylation of **6** with excess *p*-xylene dibromide gave **7**·2$PF_6$ after counter anion exchange.[37] The preparation of the diimidazolyl orthoester **11** began with an esterification of the carboxylic acid **8** to produce oxetane ester **9**.[38] This was followed by a $BF_3$-catalyzed isomerization to yield orthoester **10**,[39] which was further transformed into **11** via an Ullmann-type coupling with imidazole. The reaction between **7**·2$PF_6$ and **11** was carried out under Finkelstein-like conditions in the presence of tetrabutylammonium iodide (TBAI).[40] The resulting crude orthoester-appended macrocyclic precursor was then subject to hydrolysis in 6 N HCl[41] before being treated with excess $NH_4PF_6$. This afforded the desired monocarboxylic acid-functionalized molecular box **TxSB-$CO_2$H**·4$PF_6$ in an overall yield of 50%.

Previous work with **1**$^{4+}$ revealed that treatment with hydroxide anion could lead to irreversible imidazolium ring opening and destruction of the macrocycle.[42] Decomposition of [**TxSB-$CO_2$H**]$^{4+}$ was seen when it was treated with tetrabutylammonium hydroxide (TBAOH) in DMSO-$d_6$ or with TEA in $D_2O$ base (see ESI, Figures S17 and S18). The fully deprotonated form, **TxSB-$CO_2^-$**, could be prepared by adding two or more equivalents of TEA[22] in DMSO-$d_6$, as inferred from $^1$H NMR spectroscopic titrations (Figure S19). Precipitation of the resulting HTEA$^+$ salt was seen in most common organic solvents and in aqueous media. Therefore, DMSO and DMSO-$d_6$ were chosen as the primary solvents for studies involving **TxSB-$CO_2^-$**.

Single crystals of **TxSB-$CO_2$H** suitable for X-ray diffraction analysis were grown by slow diffusion of 2-propanol into a solution of **TxSB-$CO_2$H**·4$PF_6$ in DMSO containing a trace amount of trifluoroacetic acid (TFA). Inspection of the crystallographic data revealed that each single crystal includes five DMSO solvent molecules and four $PF_6^-$ counter anions per **TxSB-$CO_2$H** unit (*i.e.*, [**TxSB-$CO_2$H**·4$PF_6$·5DMSO]), wherein two DMSO molecules are bound to the upper and lower rims, respectively, of the macrocycle and within the cavity formed as the result of the "clip-like" conformation adopted in the solid state (Figures 1a and 1b). Two clip-like monomers pair to form a head-to-tail dimer (*i.e.*, [**TxSB-$CO_2$H**]$_2$), in which the two carboxylic acid-bearing pyridine rings, as well as the two carboxylic acid groups, are paired in an antiparallel fashion (Figures 1c, 1d, and S21). These dimers are further aggregated in the solid state to form what can be considered as dimer-based constructs of net formula {[**TxSB-$CO_2$H**]$_2$}$_n$. Presumably, this oligomeric solid state architecture is produced via a nucleation-elongation mechanism that is operative during the course of crystallization (*cf.* Figure S22). Based on considerations of stoichiometry and literature precedence involving other self-associating systems, dimerization of **TxSB-$CO_2$H** to form [**TxSB-$CO_2$H**]$_2$ is thought to constitute the first step in this nucleation and crystallization process.[43,44]

As inferred from the X-ray single crystal analysis, a combination of noncovalent interactions serve to stabilize the solid-state interlocked dimer and higher order aggregates in the solid state; these consist of: (i) hydrogen-bonding interactions between each in-cavity lower-rim-bound DMSO molecule and the carboxylic acid of a complementary **TxSB-$CO_2$H** monomer (Figure S21); (ii) a pair of π-π donor–acceptor interactions between the substituted and non-substituted pyridine rings present within each pair of macrocycles; (iii) (C–H)···O interactions between the upper-rim-bound DMSO inside each cavity and the proximal aromatic rings present in the other member of the pair (Figure S23); (iv) multiple electrostatic and (C–H)···$X^-$ interactions involving the associated $PF_6^-$ counter anions (Figure S24).

In the case of **TxSB-$CO_2^-$**, diffraction grade single crystals were obtained via the slow vapor diffusion of 2-propanol into a DMSO solution containing **TxSB-$CO_2$H**·4$PF_6$ and excess TEA. The resulting X-ray analysis revealed a structure wherein **TxSB-$CO_2^-$** adopts a "boat-like" conformation in the solid state. Two DMSO molecules and three $PF_6^-$ counter anions are found per **TxSB-$CO_2^-$** unit (*i.e.*, [**TxSB-$CO_2^-$**·3$PF_6$·2DMSO]). A single $PF_6^-$ anion is enclosed within the cavity of **TxSB-$CO_2^-$** (Figures 2a, 2b, and S25).

In the solid state, individual **TxSB-$CO_2^-$** subunits self-associate in a head-to-tail orientation to give a polymeric superstructure (*i.e.*, [**TxSB-$CO_2^-$**]$_n$). Both the cavity-bound $PF_6^-$ anion and the anionic carboxylate motifs are involved in numerous (C–H)···$X^-$ bonding interactions, which presumably play a significant role in directing the self-assembly process (Figures 2c and S26–28).

In an initial effort to determine whether the self-associated structure of **TxSB-$CO_2$H**, namely {[**TxSB-$CO_2$H**]$_2$}$_n$, or the constituent dimer, [**TxSB-$CO_2$H**]$_2$, observed in the solid state would be retained in solution, the sample as prepared (**TxSB-$CO_2$H**·4$PF_6$) was studied DMSO-$d_6$ by means of $^1$H NMR spectroscopy. One-dimensional $^1$H NMR spectra recorded as the concentration was increased from 5 to 70 mM (Figure 3a) revealed signal broadening and concentration-induced downfield shifts in the imidazolium C–H resonance $H_3$. The associated changes were plotted versus concentration and used to construct a binding isotherm. Assuming a cooperative nucleation-elongation model, an effective association constant $K_a$ of 2300 ± 400 $M^{-1}$ could be calculated via standard curve fitting (*cf.* Figure S33).[45] DOSY spectral analysis revealed a decrease in the diffusion coefficient corresponding to the $H_3$ resonance from 1.97 × $10^{-10}$ $m^2$/sec to 1.30 × $10^{-10}$ $m^2$/sec as the sample concentration was increased from 0.5 to 70 mM (Figures S29 and S32a).

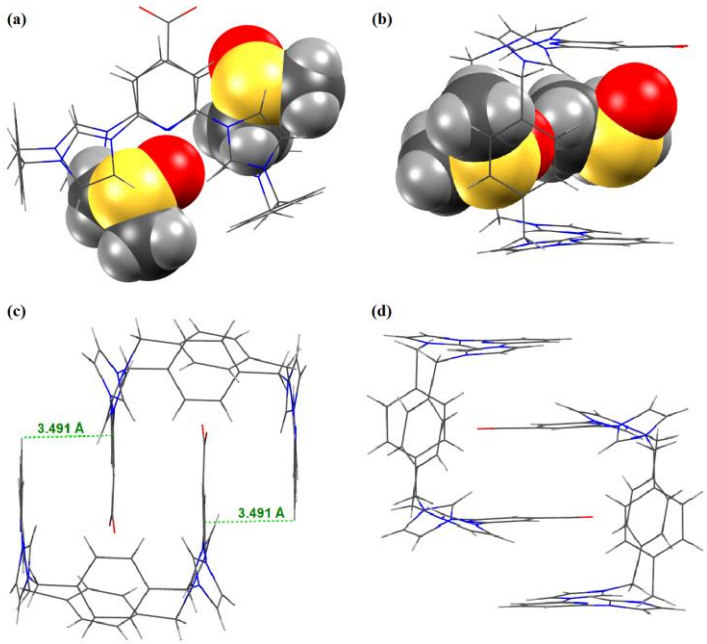


Figure 1. (a) Front and (b) side views of a single crystal X-ray diffraction structure of [**TxSB-CO$_2$H**·4PF$_6$·5DMSO] revealing a clip-like conformation for the macrocycle. Two DMSO molecules are bound within the cavity. Front (c) and side (d) views of the individual head-to-tail dimeric ensemble seen in the solid state. Some or all of the counter anions and solvent molecules have been omitted for clarity.

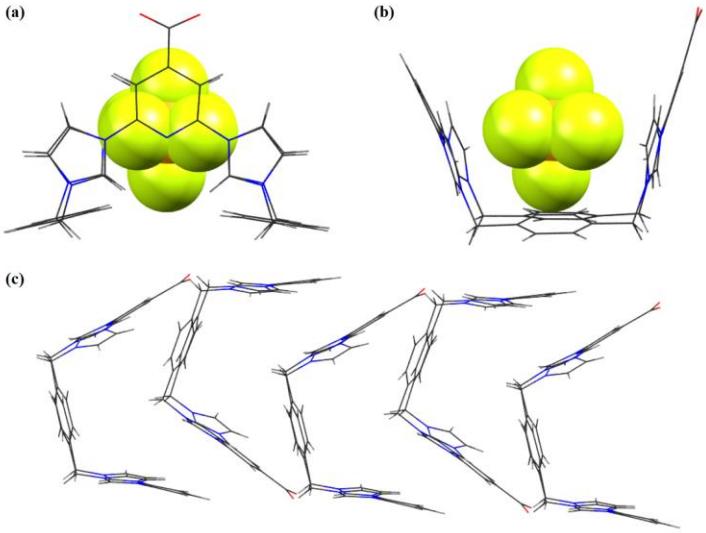


Figure 2. (a) Front and (b) side views of single crystal X-ray structure of [**TxSB-CO$_2$**·3PF$_6$·2DMSO]$^-$ showing the boat-like conformation of the carboxylate anion-functionalized macrocycle. One PF$_6^-$ counter anion is held within the macrocycle cavity and between two opposing aromatic faces. Shown in (c) is a truncated view of the head-to-tail polymeric chain structure of **TxSB-CO$_2^-$** seen in the solid state. Some or all of the counter anions and solvent molecules have been omitted for clarity.

Left undetermined by the above study was the specific nature of the interactions leading to the concentration-dependent spectral shifts and hence the determinants of the inferred self-association. Initially, they were thought to mirror the weak non-covalent effects seen in the solid state crystal structure of **TxSB-CO$_2$H** (as deduced from the metric parameters; vide supra). However, in the context of peer review, a referee noted that aggregation could arise from the presence of the basic form (**TxSB-CO$_2^-$**) produced via deprotonation in the relatively polar DMSO-$d_6$ medium. To test this possibility, a concentration dependence study analogous to that discussed above was carried out in the presence of 1% TFA-$d_1$ by weight. Now, little in the way of concentration-dependent spectral changes were observed (Figure 3b). However, a concentration-dependent DOSY analysis revealed a slight decrease in the diffusion coefficient associated with the H$_3$ resonance from 2.10 × 10$^{-10}$ m$^2$/sec at 0.5 mM to 1.51 × 10$^{-10}$

m²/sec at 70 mM (Figures S30 and S32b). We thus conclude that when **TxSB-CO₂H** is present in its fully protonated form little if any self-association occurs except possibly at the highest accessible concentrations in DMSO-$d_6$. This may reflect a lack of electrostatic interaction between the individual **TxSB-CO₂H** subunits. However, it is also possible that competition with the trifluoroacetate anion (produced as the result of solvent-induced deprotonation) limits the self-aggregation of **TxSB-CO₂H**. The solution phase behavior of **TxSB-CO₂H** thus stands in contrast to what might be inferred from the solid state structure or from an analysis of the as-prepared material in the absence of added acid.

Concentration-dependent $^1$H NMR spectroscopic analyses were also used to probe the self-association chemistry of the deprotonated form of **TxSB-CO₂H** (i.e., **TxSB-CO₂⁻**) produced from a 1:2.5 mixture of **TxSB-CO₂H** and TEA in DMSO-$d_6$. For instance, the $^1$H–$^1$H NOESY spectrum of the **TxSB-CO₂⁻** anion recorded at a concentration of 20 mM revealed a through-space coupling between $H_{11}$ and $H_{13}$. Analogous features were observed for an otherwise identical 2 mM solution (Figures 4 and S34). The correlations observed at both concentrations were fully consistent with what was inferred from the solid state structure, i.e., formation of head-to-tail polymeric ensemble [**TxSB-CO₂⁻**]$_n$ as shown in Figure 2c.

Further support for the conclusion that higher monomer concentrations favored the self-association of **TxSB-CO₂⁻** came from concentration-dependent $^1$H NMR spectroscopic studies of **TxSB-CO₂⁻** in DMSO-$d_6$ (5–70 mM) as shown in Figure 5. In analogy to what was seen in the case of the as-prepared **TxSB-CO₂H** sample, less-well resolved and broader peaks were seen over the full spectral region with in apparent downfield shifts being observed for both the imidazolium C–H resonances, of which the most downfield-shifted signal was that for $H_3$. These findings mirror what was seen previously in the case or reminiscent of the complex formed between **1**$^{4+}$ and the monoterephthalate anion, a discrete monomer that self-assembles into polyrotaxane chains.[18] By observing the concentration-dependent chemical shift changes of $H_3$ in **TxSB-CO₂⁻**, an effective equilibrium constant, $K_{eq}$, of 120 ± 2 M$^{-1}$ (Figure S35), could be calculated.[47] Based on this $K_{eq}$ value, an average degree of polymerization (*DP*) of ~5 was inferred at a concentration of 70 mM at 298 K (*cf.* ESI).[48]

A similar concentration-dependent $^1$H NMR spectral analysis of the non-functionalized Texas-sized box (**1**·4PF$_6$) was also carried out in DMSO-$d_6$ (5–70 mM). This was done as a control experiment for the above studies. In contrast to what was seen for **TxSB-CO₂⁻** but in analogy to what was observed for the fully protonated form of **TxSB-CO₂H** (i.e., studied in the presence of 1% TFA-$d_1$), no significant signal broadening and concentration-induced downfield shifts were observed in the case of **1**·4PF$_6$ (Figures S36). The difference between the parent system and both the as-prepared **TxSB-CO₂H** sample and its bona fide carboxylate anion form provides support for the conclusion that the presence of a built-in anionic functionality promotes self-association.

Addition evidence consistent with the proposed solution phase supramolecular polymerization of **TxSB-CO₂⁻** came from a series of DOSY NMR experiments. These yielded an average *DP* value of ~6 (determined using the spectral changes associated with the $H_3$ resonance) at a concentration of 70 mM at 298 K (Figures S31 and S32c).[46] The good concordance between the values obtained from the curve fits and the DOSY measurements leads to the conclusion that at relatively high, but still accessible, concentrations **TxSB-CO₂⁻** exists in the form of short self-associated oligomers in DMSO solution.

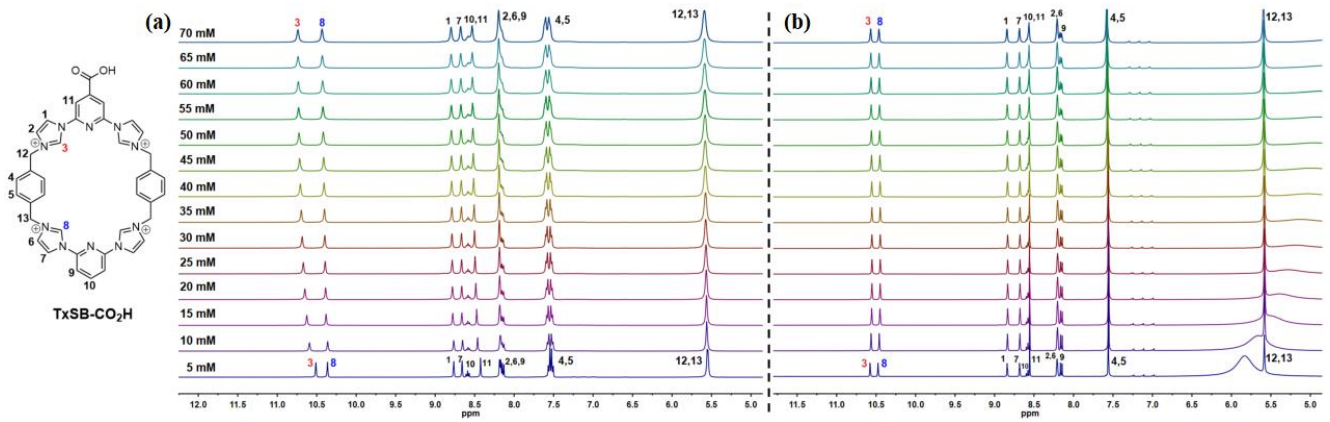


Figure 3. Concentration-dependent 400 MHz $^1$H NMR spectra of **TxSB-CO₂H**·4PF$_6$ as recorded in DMSO-$d_6$ in the absence (a) and presence of 1% TFA-$d_1$ by weight (b) at 298K (using TMS as an internal reference).

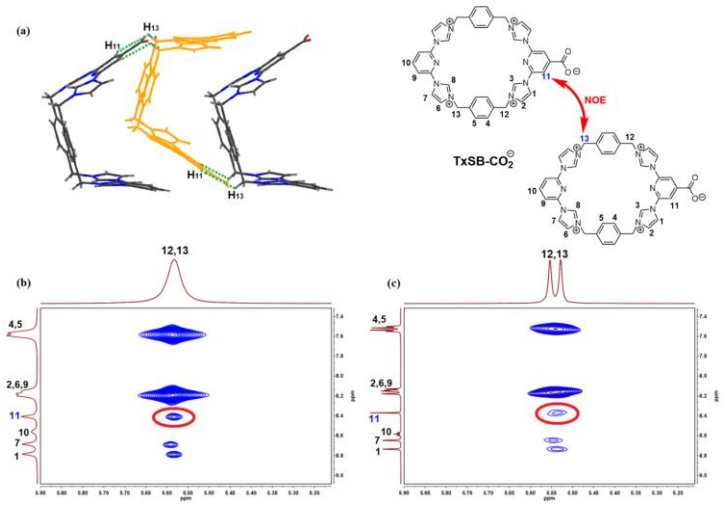


Figure 4. Truncated view (a) of the solid-state structure of [**TxSB-CO$_2^-$**]$_n$ showing the short separation (less than 3.0 Å) between the indicated protons. Expanded view (b) of the 600 MHz $^1$H–$^1$H NOESY NMR spectrum of a 20 mM solution of **TxSB-CO$_2^-$** in DMSO-$d_6$ at 298 K at the mixing time of 800 ms. The red circle present in (b) highlights the intermolecular cross-coupling between $H_{11}$ and $H_{13}$ corresponding the structural inferences drawn from (a). Such a cross-coupling peak is also seen in the NOESY NMR spectrum of 2 mM **TxSB-CO$_2^-$** under identical conditions of analysis as underscored by the red circle in (c).

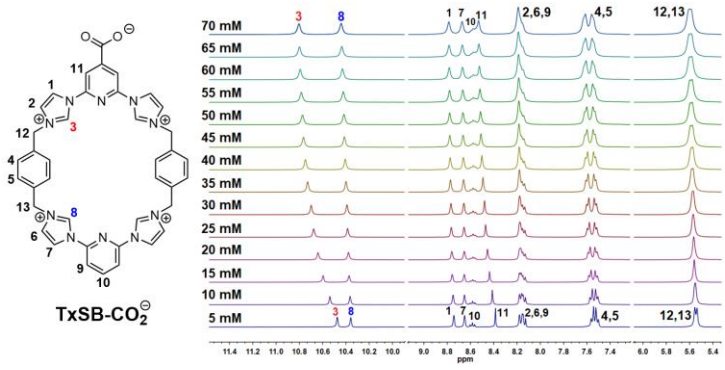


Figure 5. Concentration-dependent 400 MHz $^1$H NMR spectra of **TxSB-CO$_2^-$** recorded in DMSO-$d_6$ (containing TMS as an internal reference) at 298K.

As a complement to the $^1$H NMR spectroscopic analyses, dynamic light scattering (DLS) experiments were carried out using samples of **TxSB-CO$_2^-$**. At 20 mM an average particle size of ca. 342 nm was seen. This is a much larger value than that recorded for samples of **TxSB-CO$_2$H** containing 1% TFA at a similar concentration (particle size < 1 nm) (Figure 6). Studies of **TxSB-CO$_2^-$** were also carried out over various concentrations from 2 to 50 mM in DMSO. On the basis of these studies, two conclusions were reached. First, **TxSB-CO$_2^-$** (but not **TxSB-CO$_2$H**) is able to form and stabilize oligomeric ensembles at higher concentrations. Second, in the case of **TxSB-CO$_2^-$** (but not **TxSB-CO$_2$H**), the particle sizes were found to depend on the overall solution concentration (cf. Figure S37 in the ESI). This is in a good agreement with our findings from the one- and two-dimensional $^1$H NMR spectroscopic studies discussed above.

To gain further insights into the reversible nature of the self-associated oligomers formed from **TxSB-CO$_2^-$**, variable-temperature (VT) $^1$H NMR spectroscopic studies were carried out. For a 20 mM (DMSO-$d_6$) solution of **TxSB-CO$_2^-$**, the peaks became sharper and appear well-resolved across the full spectrum as the temperature was raised. Upfield shifts were seen for many of the resonances, with the effect being greatest for the imidazolium C–H protons (Figure S38). Such findings are consistent with a system that undergoes thermal-based disaggregation. This is as expected for a **TxSB-CO$_2^-$**-based oligomer stabilized at room temperature via noncovalent (C–H)...X$^-$ interactions.[22] Additional VT NMR spectra were recorded at 2 mM under the same analytical conditions. Similar spectral changes were observed at this lower concentration (Figures 38b). This latter finding provides further support for the contention that multiple oligomer-stabilizing intermolecular interactions are retained at lower concentra-

tions at room temperature and that the resulting self-associated species (i.e., [**TxSB-CO$_2^-$**]$_n$) dissociate as the temperature is raised.

Further support for the reversible nature of the self-assembled oligomers produced from **TxSB-CO$_2^-$** came from pH-dependent $^1$H NMR spectroscopic analyses. Here, it was found that, upon addition of 2.5 equivalents of TEA to a DMSO-$d_6$ solution containing **TxSB-CO$_2$H** at a concentration of 20 mM, the resonances assigned to $H_3$, $H_8$, and $H_{4/5}$ (where $H_{4/5}$ refers to an overlapping signal ascribed to $H_4$ and $H_5$) within the macrocycle shift to lower field. Based on these observations, we surmise that, under these conditions, **TxSB-CO$_2$H** undergoes deprotonation to form **TxSB-CO$_2^-$**, a transformation that is followed by self-association to form [**TxSB-CO$_2^-$**]$_n$. Increasing the acidity of the resulting solution (containing [**TxSB-CO$_2^-$**]$_n$), via the addition of 5.0 equivalents of deuterated trifluoracetic acid (TFA-$d_1$), was found to protonate **TxSB-CO$_2^-$** and thus disassemble [**TxSB-CO$_2^-$**]$_n$ to regenerate **TxSB-CO$_2$H**. Evidence for this transformation came from the observation that the chemical shifts of the $H_3$, $H_8$, and $H_{4/5}$ signals reverted to their original positions upon protonation. The subsequent addition of TEA and led to restoration of spectra features ascribable to [**TxSB-CO$_2^-$**]$_n$. The process could be repeated via the subsequent additions of acid and base, thus allowing interconversion between **TxSB-CO$_2$H** and [**TxSB-CO$_2^-$**]$_n$. However, with each addition of acid or base, the background salt concentration increases. This leads to a "dampening" of the interconversion effect with each cycle. Nevertheless, it proved possible to repeat the interconversion between [**TxSB-CO$_2^-$**]$_n$ and **TxSB-CO$_2$H** a number of times (*cf.* Figure 7).[22]

In addition to modulating the aggregation behavior of **TxSB-CO$_2^-$** through changes in temperature, pH, and concentration, we considered it likely that disassociation could be promoted via the addition of a competitive anion. Support for this postulate came from recent studies by Gong *et al.*,[50] wherein it was found that the formate and benzoate anions formed complexes with the parent (unfunctionalized) macrocycle **1**$^{4+}$. In the present instance, it was found that addition of 1 molar equiv of tetrabutylammonium acetate (TBAOAc) to a 20 mM solution of the anionic forms of **TxSB-CO$_2^-$** in DMSO-$d_6$ led to discernible changes in the $^1$H and $^1$H–$^1$H NOESY NMR spectra (Figure S39a). A similar addition led to changes in the $^1$H–$^1$H NOESY NMR spectrum of as-prepared samples of **TxSB-CO$_2$H**, as would be expected given the weakly basic nature of the OAc$^-$ anion (Figure S39b). No such spectral changes were seen when acetic acid was added to a 20 mM DMSO-$d_6$ solution of **TxSB-CO$_2$H**.

In the case of **TxSB-CO$_2^-$** and the acetate anion, a $^1$H NMR spectroscopic Job plot was constructed. On this basis, a 1:3 (host-guest) complex stoichiometry was inferred (Figure S40).[49] This stoichiometry is consistent with the presence of multiple interactions between the acetate anions and the Texas box receptor. Support for this latter inferences came from the observation of $^1$H–$^1$H couplings between the acetate anion and various **TxSB-CO$_2^-$** protons in the NOESY spectrum (cf. Figure S39a).

Further support for the suggestion that the acetate anion can be used to dissemble the self-associated form of **TxSB-CO$_2^-$** came from DLS analyses. As can be seen from an inspection of Figure 6c, a mean particle diameter of ca. 342 nm was deduced for DMSO solutions of **TxSB-CO$_2^-$** at a concentration of 20 mM on the basis of DLS analyses. In contrast, mixed solutions containing 1:1 TBAOAc–**TxSB-CO$_2^-$** at 20 mM in both species produced particles with a relatively small average diameter of 18 nm as judged from analogous DLS studies.

The ability of the acetate anion to induce deaggregation was also probed by means of scanning electron microscopy (SEM).[50] Consistent with the crystallographic analyses and what was inferred from the DLS studies, rod-like nanostructures were seen for the solid-phase aggregates obtained from **TxSB-CO$_2^-$** (*cf.* Figure 8a). In contrast, relatively small sized granular assemblies were found in the SEM samples made up from a 1:1 mixture of TBAOAc and **TxSB-CO$_2^-$** (*cf.* Figure 8b). On the basis, we propose that the acetate anion provides an external stimulus that can be used to control the self-association features of **TxSB-CO$_2^-$**. The acetate anion could thus provide a potential complement to other modulators, such as temperature, pH, and concentration.

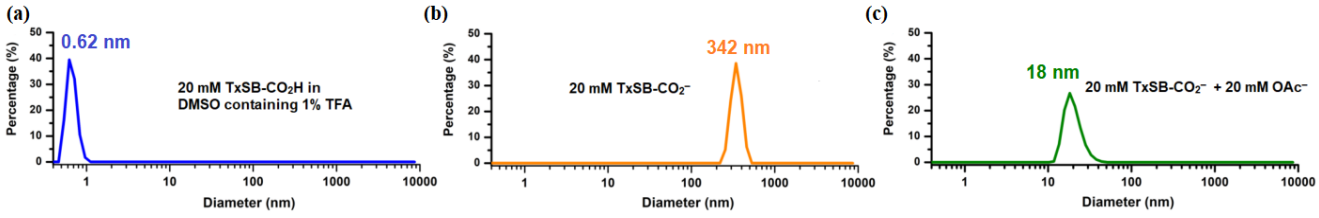


Figure 6. DLS size distributions of 20 mM DMSO solutions of (a) **TxSB-CO$_2$H** in the presence of 1% TFA by weight, (b) **TxSB-CO$_2^-$**, and (c) an equimolar mixture of **TxSB-CO$_2^-$** and TBAOAc. All analyses were carried out at room temperature.

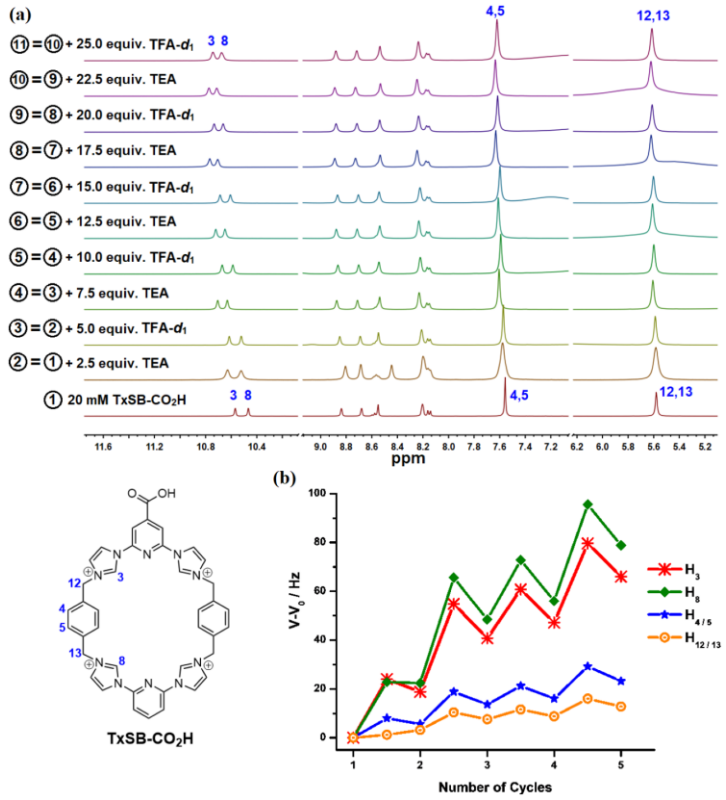


Figure 7. (a) pH-dependent 400 MHz $^1$H NMR spectroscopic studies of **TxSB-CO$_2$H** carried out at a receptor concentration of 20 mM in DMSO-$d_6$ at 298 K. (b) Changes in resonance frequencies of selected macrocycle protons as specified in the inset were used to monitor the pH-switchable interconversion between [**TxSB-CO$_2$H**]$_2$ and [**TxSB-CO$_2^-$**]$_n$.

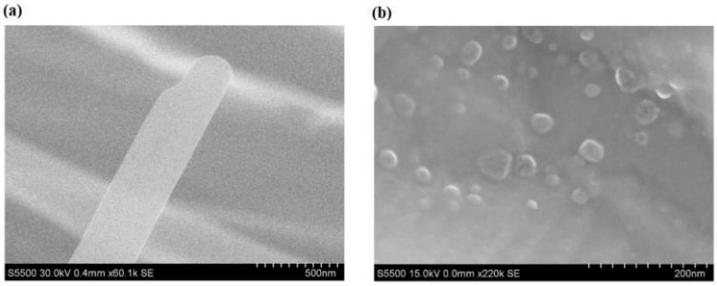


Figure 8. SEM images of the granular and rod-like assemblies obtained from separate solution samples prepared from (a) **TxSB-CO$_2^-$** and (b) an equimolar mixture of **TxSB-CO$_2^-$** and TBAOAc (scale bars = 500 or 200 nm).

## CONCLUSIONS

In summary, a carboxylic acid-functionalized Texas-sized molecular box **TxSB-CO$_2$H** was designed and synthesized. While this new derivative was seen to self-associate to produce an extended array of dimers in the solid state, concentration-dependent $^1$H NMR spectroscopic studies revealed little evidence of aggregation except possibly at the highest concentrations accessible in DMSO-$d_6$ as long as the acid moiety was in its fully protonated form. The appended carboxylic acid group (tail unit) present in **TxSB-CO$_2$H** can be effectively converted into its conjugate base, **TxSB-CO$_2^-$**, by treatment with TEA in DMSO or DMSO-$d_6$. Such an alteration in the tail functionality leads to the production of self-complementary monomers, **TxSB-CO$_2^-$**. These anion-containing monomers associate into a higher-order head-to-tail oligomers [**TxSB-CO$_2^-$**]$_n$ in solution and in the solid state. These self-assembled structures were characterized on the basis of one- and two-dimensional $^1$H NMR spectroscopic studies carried out in DMSO-$d_6$, single crystal X-ray diffraction analyses, DLS measurements, and SEM imaging. The ensembles produced from **TxSB-CO$_2^-$**

proved to be environmentally responsive, with the extent of assembly being readily modulated via changes in temperature, pH, and concentration, as well as via the addition of the acetate anion as a competitive guest. The present work shows how ostensibly similar receptors can be used to create very different kinds of solution phase and solid state structures. As such, it could set the stage for the design and synthesis of more sophisticated supramolecular systems, such as so-called smart materials[26,33] and molecular level switches,[15,17] that would benefit from the availability of large cationic macrocyclic building blocks. The present work also serves to underscore how structures inferred from solid state structural analyses are not necessarily reflective of the forms that dominate in competitive solution phase media.

## ASSOCIATED CONTENT

Supporting Information: Synthetic details, crystallographic elucidations, NMR isotherm curve-fitting, and other spectroscopic data. Cif file for TxSB-$CO_2H$ (CCDC 1573263); cif file for TxSB-$CO_2^-$ (CCDC 1573264). This material is available free of charge via the Internet at http://pubs.acs.org.

## AUTHOR INFORMATION

### Corresponding Author

*sessler@cm.utexas.edu

ORCID numbers:
Ren-Tsung Wu: 0000-0003-4830-8963
Xiaodong Chi: 0000-0002-6726-8584
Takehiro Hirao: 0000-0003-4377-7541
Vincent M. Lynch: 0000-0002-5260-9913
Jonathan L. Sessler: 0000-0002-9576-1325

### Notes

The authors declare no competing financial interest.

## ACKNOWLEDGMENT

The work in Austin was supported by the National Institutes of Health (RGM 103790A to J.L.S.) and the Robert A. Welch Foundation (F-0018).

## REFERENCES

(1) Schmidtchen, F. P.; Berger, M. *Chem. Rev*. **1997**, *97*, 1609–1646.
(2) Beer, P. D.; Gale, P. A. *Angew. Chem. Int. Ed*. **2001**, *40*, 486–516.
(3) Steed, J. W.; Atwood, J. L. *Supramolecular Chemistry*, 2nd ed.; Wiley & Sons: Chichester, UK, 2009; pp. 308–382.
(4) Kim, S. K.; Sessler, J. L. *Acc. Chem. Res.* **2014**, *47*, 2525–2536.
(5) Liu, Z.; Nalluri, S. K. M.; Stoddart, J. F. *Chem. Soc. Rev.* **2017**, *46*, 2459–2478.
(6) Odell, B.; Reddington, M. V.; Slawin, A. M. Z.; Spencer, N.; Stoddart, J. F.; Williams, D. J. *Angew. Chem. Int. Ed.* **1988**, *27*, 1547–1550.
(7) Amabilino, D. B.; Stoddart, J. F. *Pure Appl. Chem*. **1996**, *68*, 2351–2359.
(8) Langford, S. J.; Stoddart, J. F. *Pure Appl. Chem*. **1996**, *68*, 1255–1260.
(9) Dale, E. J.; Vermeulen, N. A.; Juríček, M.; Barnes, J. C.; Young, R. M.; Wasielewski, M. R.; Stoddart, J. F. *Acc. Chem. Res.* **2016**, *49*, 262–273.
(10) Raymo, F. M.; Stoddart, J. F. *Chem. Rev.* **1999,** *99,* 1643–1664.
(11) Barin, G.; Coskun, A.; Fouda, M. M. G.; Stoddart, J. F. *ChemPlusChem* **2012**, *77*, 159–185.
(12) Young, R. M.; Dyar, S. M.; Barnes, J. C.; Juríček, M.; Stoddart, J. F.; Co, D. T.; Wasielewski, M. R. *J. Phys. Chem. A* **2013**, *117*, 12438–12448.
(13) Dyar, S. M.; Barnes, J. C.; Juríček, M.; Stoddart, J. F.; Co, D. T.; Young, R. M.; Wasielewski, M. R. *Angew. Chem. Int. Ed.* **2014**, *53*, 5371–5375.
(14) Flood, A. H.; Stoddart, J. F.; Steuerman, D. W.; Heath, J. R. *Science* **2004**, *306*, 2055–2056.
(15) Stoddart, J. F. *Chem. Soc. Rev.* **2009**, *38*, 1802–1820.
(16) Balzani, V.; Gómez-López, M.; Stoddart, J. F. *Acc. Chem. Res.* **1998**, *31*, 405–414.
(17) Erbas-Cakmak, S.; Leigh, D. A.; McTernan, C. T.; Nussbaumer, A. L. *Chem. Rev*. **2015**, *115*, 10081–10206.
(18) Gong, H. -Y.; Rambo, B. M.; Karnas, E.; Lynch, V. M.; Sessler, J. L. *Nat. Chem.* **2010**, *2*, 406–409.
(19) Gong, H. -Y.; Rambo, B. M.; Lynch, V. M.; Keller, K. M.; Sessler, J. L. *J. Am. Chem. Soc*. **2013**, *135*, 6330–6337.
(20) Yang, Y. -D.; Sessler. J. L.; Gong, H. -Y. *Chem. Commun.* **2017**, *53*, 9684–9696.
(21) Gong, H. -Y.; Rambo, B. M.; Lynch, V. M.; Keller, K. M.; Sessler, J. L. *Chem. –Eur. J.* **2012**, *18*, 7803–7809.
(22) Gong, H. -Y.; Rambo, B. M.; Karnas, E.; Lynch, V. M.; Keller, K. M.; Sessler, J. L. *J. Am. Chem. Soc*. **2011**, *133*, 1526–1533.
(23) Rambo, B. M.; Gong, H. -Y.; Oh, M.; Sessler, J. L. *Acc. Chem. Res.* **2012**, *45*, 1390–1401.
(24) Wang, C. -L.; Zhou, L.; Zhang, L.; Xiang, J. -F.; Rambo, B. M.; Sessler, J. L.; Gong, H. -Y. *Chem. Commun*. **2017**, *53*, 3669–3672.
(25) Silver, E. S.; Rambo, B. M.; Bielawski, C. W.; Sessler, J. L. *J. Am. Chem. Soc*. **2014**, *136*, 2252–2255.
(26) Yang, L.; Tan, X.; Wang, Z.; Zhang, X. *Chem. Rev.* **2015**, *115*, 7196–7239.
(27) Takashima, Y.; Harada, A. *J. Incl. Phenom. Macrocycl. Chem*. **2017**, *88*, 85–104.
(28) Gyarmati, B.; Szilágyi, B. Á.; Szilágyi, A. *Eur. Polym. J.* **2017**, *93*, 642–669.
(29) Sessler, J. L.; Andrievsky, A.; Gale, P. A.; Lynch, V. M. *Angew. Chem. Int. Ed.* **1996**, *35*, 2782–2785.
(30) Ashton, P. P.; Parsons, I. W.; Raymo, F. M.; Stoddart, J. F.; White, A. J. P.; Williams, D. J.; Wolf, R. *Angew. Chem. Int. Ed.* **1998**, *37*, 1913–1916.
(31) Cao, D.; Wang, C.; Giesener, M. A.; Liu, Z.; Stoddart, J. F. *Chem. Commun.* **2012**, *48*, 6791–6793.
(32) Rotzler J.; Mayor, M. *Chem. Soc. Rev.* **2013**, *42*, 44–62.
(33) Bruns, C. J.; Stoddart, J. F. *Acc. Chem. Res.* **2014**, *47*, 2186–2199.
(34) Kim, D. S.; Chang, J.; Leem, S.; Park, J. S.; Thordarson, P.; Sessler, J. L. *J. Am. Chem. Soc.*, **2015**, *137*, 16038–16042.
(35) Ji, X.; Wang, H.; Li, Y.; Xia, D.; Li, H.; Tang, G.; Sessler, J. L.; Huang, F. *Chem. Sci*. **2016**, *7*, 6006–6014.
(36) Walter, S. M.; Kniep, F.; Herdtweck, E.; Huber S. M. *Angew. Chem. Int. Ed.* **2011**, *50*, 7187–7191.
(37) Ashton, P. R.; Ballardini, R.; Balzani, V.; Bělohradský, M.; Gandolfi, M. T.; Philp, D.; Prodi, L.; Raymo, F. M.; Reddington, M. V.; Spencer, N.; Stoddart, J. F.; Venturi, M.; Williams, D. J. *J. Am. Chem. Soc.* **1996**, *118*, 4931–4951.
(38) Rose, N. G. W.; Blaskovich, M. A.; Wong, A.; Lajoie, G. A. *Tetrahedron* **2001**, *57*, 1497–1507.

(39) Choony, N.; James, L.; Rabun, C. *Synthetic Commun.* **2001**, *41*, 2539–2543.
(40) Barnes, J. C.; Juríček, M.; Vermeulen, N. A.; Dale, E. J.; Stoddart, J. F. *J. Org. Chem*. **2013**, *78*, 11962–11969.
(41) Luo, Y.; Blaskovich, M. A.; Lajoie, G. A *J. Org. Chem*. **1999**, *64*, 6106–6111.
(42) Shang, J.; Rambo, B. M.; Hao, X.; Xiang, J.-F.; Gong, H.-Y.; Sessler, J. L. *Chem. Sci*. **2016**, *7*, 4148–4157.
(43) Zhao, D.; Moore, J. S. *Org. Biomol. Chem*. **2003** , *1*, 3471–3491.
(44) Mahadevi, A. S.; Sastry, G. N. *Chem. Rev.* **2016**, *116*, 2775–2825.
(45) Wackerly, J. W.; Moore, J. S. *Macromolecules* **2006**, *39*, 7269–7276.
(46) Schmidt, R.; Stolte, M.; Grüne, M.; Würthner, F. *Macromolecules* **2011**, *44*, 3766–3776.
(47) Martin, R. B. *Chem. Rev*. **1996**, *96*, 3043–3064.
(48) Xu, J.; Fogleman, E. A.; Craig, S. L. *Macromolecules* **2004**, *37*, 1863–1870.
(49) Tang, F.; Cao, R.; Gong, H. -Y.; *Tetrahedron Lett*. **2015**, *56*, 820–823.
(50) Zhang, H.; Lee, J.; Lammer, A. D. Chi, X.; Brewster, J. T.; Lynch, V. M.; Li, H.; Zhang, Z.; Sessler, J. L. *J. Am. Chem. Soc*. **2016**, *138*, 4573–4579.

**TOC Graphic:**

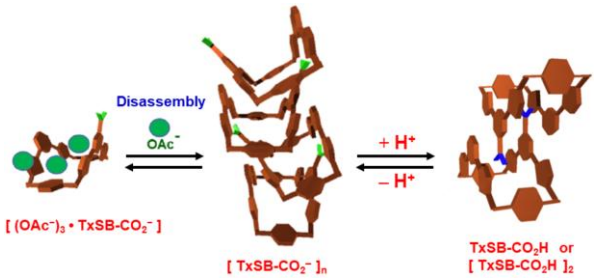
Disassembly
OAc⁻
+ H⁺
– H⁺
[ (OAc⁻)₃ • TxSB-CO₂⁻ ]
[ TxSB-CO₂⁻ ]n
TxSB-CO₂H or
[ TxSB-CO₂H ]₂